J. Fluid Mech. (1980), *vol.* 98, *part* 1, *pp.* 137–148
Printed in Great Britain

Effect of departures from the Oberbeck–Boussinesq approximation on the heat transport of horizontal convecting fluid layers

By GUENTER AHLERS

Bell Laboratories, Murray Hill, New Jersey 07974

(Received 9 May 1979 and in revised form 31 August 1979)

Measurements are presented of the Nusselt numbers N and Rayleigh numbers R for shallow layers of ^{4}He gas heated from below. By choosing different temperatures between 2·3 K and 5·1 K and different pressures between 0·07 bar and 1 bar, the extent Q of departures from the Oberbeck–Boussinesq approximation was varied. When R was evaluated at the static temperature at the midplane of the cell, both the critical Rayleigh number R_c and the initial slope N_1 of the Nusselt number were found to be independent of Q within experimental scatter. This result agrees with the prediction of Busse (1967). When R was evaluated at the cold end temperature of the cell, both R_c and N_1 depended strongly upon Q.

1. Introduction

The problem of convection in a fluid contained between horizontal parallel plates and heated from below is usually discussed within the framework of the approximation of Oberbeck (1879) and of Boussinesq (1903) (OB).† In this approximation, the temperature dependences of fluid properties are neglected, except for thermally induced density differences when they induce buoyant forces. Real fluids virtually never conform fully to this approximation, although they may come close. It is therefore of some practical interest for the interpretation of experimental measurements to study systematically how non-OB effects manifest themselves in real systems. In addition, these effects are of course of considerable intrinsic interest, and a good deal of theoretical attention has been devoted to them. However, there has been relatively little experimental work on this problem. The experiments that have been performed have concentrated primarily upon visual observations of the convective flow patterns (Somerscales & Dougherty 1970; Hoard, Robertson & Acrivos 1970), although recently rather quantitative local measurements of the fluid velocity were performed for the somewhat extreme case where the expansion coefficient vanishes at the top of the cell and is finite at the bottom (Dubois, Berge & Westfried 1978).

In this paper, quantitative measurements of heat transport by the convecting fluid are presented. The measurements were made, using ^{4}He gas as the fluid, at a number of different densities and temperatures. By changing the point in the phase diagram at which measurements were made, it was possible to vary continuously the extent of the departures from the OB approximation and thus to study any non-OB effects

† For an informative historical comment on the OB approximation, see Joseph (1971).

systematically. However, we are concerned here only with moderately non-OB systems, and the data to be presented do not address themselves to the hysteretic phenomena which are expected to occur near the critical Rayleigh number R_c in very non-OB cases (Busse 1967). Rather, it is the purpose of the present work to provide precision measurements of R_c, and of the Nusselt number N for R greater than but near R_c, for small to moderate departures from the OB approximation.

Since the fluid properties of a non-OB system depend upon the temperature, the Rayleigh number is not unique but rather depends upon the vertical position within the cell. It was predicted by Busse (1967) that R_c will be independent (to first order) of the departures from the OB approximation if it is evaluated at the static temperature T_{s0} at the horizontal midplane ($z = 0$) of the convection cell. The data to be presented are in excellent agreement with this prediction. They also show that the dependence of the Nusselt number upon the Rayleigh number for $R > R_c$ is not measurably influenced by non-OB effects if R is evaluated at T_{s0}.

Some of the results presented in this paper have been reported briefly elsewhere (Ahlers 1974, 1975).

2. Apparatus and procedure

The apparatus used for this work has been described adequately elsewhere (Ahlers 1971, 1978), and only the main features are summarized here. The convection cell had a circular cross-section with a diameter D of 0·927 cm and a height h of 0·086 ± 0·003 cm. Uncertainties in the Rayleigh numbers (see equation 4.1 below) due to the uncertainty in h therefore are no larger than 10 %. Lateral variations in the height were no more than 3 % and caused a small amount of rounding of the Nusselt number near the onset of convection. During the measurements, the temperature at the top of the fluid was held constant, and a heat current was introduced at the bottom. Both top and bottom plates were made of copper, which had a thermal conductivity at least four orders of magnitude greater than that of the fluid. Thus, extremely uniform temperatures along the horizontal boundaries were assured.

The measurements were made over the temperature range from 2·3 to 5·1 K and at pressures between 0·07 and 1 bar.

For $R < R_c$, the applied heat current q and measured steady-state temperature difference ΔT yielded the thermal conductivity λ of the fluid. Corrections for the wall conduction l_w were made by using the equation

$$\lambda = (q/\Delta T - l_w)\, h/A, \tag{2.1}$$

where A is the cross-sectional area. The ratio of the conductance l_{fl} of the fluid to that of the wall depended mildly upon the temperature, but typically was 1·18. For $R > R_c$, an effective thermal conductivity λ_{eff} was derived from (2.1) and the measurements, and the Nusselt number N was given by $\lambda_{\mathrm{eff}}/\lambda$. Since λ is dependent upon ΔT for the non-OB fluid, we chose $\lambda(\bar{T})$ for the normalization of N. Here $\bar{T}$ is the mean temperature.

Possible effects of the relatively large wall conduction upon the Nusselt number were explored by making measurements using *liquid* helium as the fluid. In that case, l_{fl} is considerably larger, and $l_{\mathrm{fl}}/l_{\mathrm{w}}$ can be as large as 7. The results for $N(R)$ were indistinguishable from those obtained using ^{4}He gas.

3. Fluid properties

In order to derive Rayleigh numbers from the measured temperature differences, it is necessary to have an equation of state, and to know the viscosity and the thermal conductivity.

The virial equation of state

$$PV = RT(1+B/V) \tag{3.1}$$

with the second virial coefficient given by (Keller 1969)

$$B = \alpha+\beta/T, \tag{3.2}$$

where $\alpha = 23{\cdot}05\,\mathrm{cm^3\,mol^{-1}}$, and $\beta = -421{\cdot}2\,\mathrm{K\,cm^3\,mol^{-1}}$, is sufficiently accurate over the pressure and temperature range of this investigation. In equation (3.1), P is the pressure, V the molar volume, T the absolute temperature, and $R = 83{\cdot}1432\,\mathrm{cm^3\,bar\,mol^{-1}\,K^{-1}}$ is the gas constant. From equation (3.1), we obtain

$$V = \frac{RT}{2P}\left[1+\left(1+\frac{4PB}{RT}\right)^{\frac{1}{2}}\right]. \tag{3.3}$$

The density is given by

$$\rho = 4{\cdot}0038/V. \tag{3.4}$$

A comparison of the density derived from these equations and the measured density of the gas at saturated vapour pressure has been given elsewhere (Ahlers 1978), and the agreement is very good.

For the isobaric thermal expansion coefficient we have

$$\begin{aligned}\beta_P &\equiv V^{-1}(\partial V/\partial T)_P \\ &= T^{-1}+V^{-1}(B'-B/T)/(1+4BP/RT)^{\frac{1}{2}},\end{aligned} \tag{3.5}$$

where

$$\begin{aligned}B' &= dB/dT \\ &= -\beta/T^2.\end{aligned}$$

The heat capacity at constant pressure can be derived also from (3.1), and is given by

$$C_P = \frac{3R}{2}+\frac{RT}{V}\left[V\beta_P\left(1+\frac{B}{V}+\frac{B'T}{V}\right)-2B'-TB''\right], \tag{3.6}$$

where

$$B'' = 2\beta/T^3.$$

The thermal conductivity was measured during this work, using thermal gradients sufficiently small to avoid convection (Ahlers 1978). In the low-density limit, these results are in good agreement with those of Kerrick & Keller (1969).

The shear viscosity η was determined by Becker, Misenta & Schmeissner (1954*a*, *b*), and their data can be represented by

$$\eta = -0{\cdot}51+2{\cdot}68T, \tag{3.7}$$

where η is in μP

4. Theoretical predictions

The Rayleigh number is defined as

$$R \equiv \frac{g\beta_P(T_1 - T_2)\,h^3}{\kappa\nu}, \tag{4.1}$$

where g is the gravitational acceleration, h the height of the fluid layer, $\kappa = \lambda/\rho C_P$ the thermal diffusivity, $\nu = \eta/\rho$ the kinematic viscosity, and T_1 and T_2 are the temperatures at the bottom and top of the cell respectively. The vertical axis is z, and the top and bottom boundaries are at $z = \frac{1}{2}$ and $z = -\frac{1}{2}$ respectively. For the non-OB system, R depends upon z because β_P, κ and ν depend upon $T(z)$. The second relevant dimensionless parameter in the problem is the Prandtl number, given by

$$\sigma = \nu/\kappa. \tag{4.2}$$

The z dependence of σ is very weak because ν and κ have a similar temperature dependence. The value of σ is always close to $\frac{2}{3}$, as expected for a gas in the low density limit (Hirschfelder, Curtiss & Bird 1954).

The effect of departures from the Oberbeck–Boussinesq approximation for a laterally infinite fluid has been discussed by a number of authors, including Busse (1962, 1967), Palm, Ellingsen & Gjevik (1967) and Davis & Segel (1968). Of these, the results by Busse (1967) are the most complete in the sense that they consider (to first order) the effect of variations in all the relevant fluid properties, and the effect of finite Prandtl numbers.

We shall therefore compare the experimental results with these theoretical predictions, although one must keep in mind that the experiments pertain to a laterally finite system. Busse defined the parameter†

$$Q \equiv \sum_{i=0}^{4} \gamma_i P_i \tag{4.3}$$

to describe the extent of departures from the OB approximation. Here

$$\gamma_0 = -(\rho_1 - \rho_2)/\rho_0, \tag{4.4a}$$

$$\gamma_1 = (\beta_{P1} - \beta_{P2})/2\beta_{P0}, \tag{4.4b}$$

$$\gamma_2 = (\nu_1 - \nu_2)/\nu_0, \tag{4.4c}$$

$$\gamma_3 = (\lambda_1 - \lambda_2)/\lambda_0, \tag{4.4d}$$

$$\gamma_4 = (C_{P1} - C_{P2})/C_{P0}. \tag{4.4e}$$

The subscripts 1 and 2 indicate that the fluid properties should be evaluated at the temperatures T_1 and T_2, corresponding to $z = -\frac{1}{2}$ and $z = \frac{1}{2}$, respectively. The subscript 0 indicates that a reference temperature T_0 is used. The parameters P_i are (Busse 1967)

$$P_0 = 2{\cdot}676 - 0{\cdot}1258/\sigma, \tag{4.5a}$$

$$P_1 = -6{\cdot}603 - 0{\cdot}5023/\sigma, \tag{4.5b}$$

$$P_2 = 2{\cdot}755 + 0/\sigma, \tag{4.5c}$$

$$P_3 = 2{\cdot}917 - 0{\cdot}5023/\sigma, \tag{4.5d}$$

$$P_4 = -6{\cdot}229 + 0{\cdot}2512/\sigma. \tag{4.5e}$$

† Our parameter Q is the same as Busse's (1967) P. We reserve the symbol P to denote the pressure.

In the last equations, the constant terms were calculated for rigid–rigid boundary conditions, but the coefficients of the σ^{-1} terms are approximate and taken from calculations for free–free boundary conditions.

For non-zero Q, the theory predicts that the critical Rayleigh number $R_c(z)$ will be independent of Q (to linear order) only at $z = 0$. When the thermal conductivity varies linearly with T, the static temperature $T_s(z)$ is given by†

$$T_s(z) = \tfrac{1}{2}(T_1+T_2)+(T_2-T_1)\,[z+(\tfrac{1}{2}\gamma_3)\,(z^2-\tfrac{1}{4})], \tag{4.6}$$

and at $z = 0$ it has the value

$$\begin{aligned} T_{s0} &= T_s(0) \\ &= \tfrac{1}{2}(T_1+T_2)+\tfrac{1}{8}(T_1-T_2)\,\gamma_3. \end{aligned} \tag{4.7}$$

We define a Rayleigh number R_0 in terms of equation (4.1) and the fluid properties at T_{s0}. In the next section we shall examine the experimental results for the critical value R_{c0} of R_0. In addition to the critical Rayleigh number R_{c0}, there are three distinguished values of R_0, to be referred to as R_A, R_R, and R_B, with

$$R_A < R_{c0} < R_R < R_B.$$

For $R_A < R_0 < R_R$, only flow of hexagonal symmetry is stable according to the theory. For $R_R < R_0 < R_B$, both hexagonal flow and the rolls characteristic of the OB approximation are predicted to be stable. For $R_0 > R_B$, only rolls remain stable. The transitions are given by

$$(R_A-R_{c0})/Q^2 = -1/4R_H^{(20)}, \tag{4.8}$$

$$(R_B-R_{c0})/Q^2 = (9R_H^{(20)}-3L_2)/L_2^2, \tag{4.9}$$

$$(R_R-R_{c0})/Q^2 = 3R_R^{(20)}/L_2^2, \tag{4.10}$$

with‡

$$R_H^{(20)} = 0{\cdot}89360+0{\cdot}04959/\sigma+0{\cdot}06787/\sigma^2, \tag{4.11}$$

$$R_R^{(20)} = 0{\cdot}69942-0{\cdot}00472/\sigma+0{\cdot}00832/\sigma^2, \tag{4.12}$$

$$L_2 = 0{\cdot}29127+0{\cdot}08147/\sigma+0{\cdot}08933/\sigma^2. \tag{4.13}$$

The convective heat transport for the hexagons (for $R_A < R_0 < R_B$) is given by

$$\overline{H}_H = \frac{R_0-R_{c0}}{R_H^{(20)}}+\frac{Q^2}{2(R_H^{(20)})^2}+\frac{|Q|}{2R_H^{(20)}}\left[\frac{Q^2}{(R_H^{(20)})^2}+\frac{4(R_0-R_{c0})}{R_H^{(20)}}\right]^{\frac{1}{2}}. \tag{4.14}$$

For the rolls, the OB result (Schlüter, Lortz & Busse 1965)

$$\overline{H}_R = (R_0-R_{c0})/R_R^{(20)} \tag{4.15}$$

applies. The Nusselt number is related to $\overline{H}$ by $N = 1+\overline{H}/R_0$. Equation (4.14) indicates that near R_{c0} the deviation of N from the OB value is of order Q^2/R_{c0}. Therefore it appears that the results of the theory should apply when $Q^2 \ll R_{c0}$. For the present work, this condition is always satisfied. Values of Q pertinent to the data are given in table 1.

† Equation (6.6) of Busse (1967) for T_s contains misprints.

‡ The parameters $R_H^{(20)}$ and $R_R^{(20)}$ differ from the parameters $R_H^{(2)}$ and $R_R^{(2)}$ given by Schlüter *et al.* (1965) by the factor $\sigma/K = 1/2904{\cdot}4$ of that reference.

Sample	T_2 [K]	P [mbar]	$(T_1-T_2)_c$ [K]	σ	R_{c0}	N_{10}	N_{20}	Q_c
1	2·3768	67·90	0·1564	0·73	1746	—	—	1·06
2	2·9399	84·90	0·3944	0·70	1741	0·868	−0·26	1·93
5	3·2883	95·44	0·7561	0·69	(1758)	—	—	2·66
6	3·2883	116·0	0·3579	0·70	1790	—	—	1·58
7	3·2883	136·6	0·2166	0·70	1774	0·906	−0·30	1·05
8	3·2883	158·3	0·1438	0·71	1770	0·892	−0·28	0·72
9	3·2883	187·8	0·0918	0·72	(1788)	—	—	0·50
10	3·2883	204·7	0·0724	0·72	1782	0·909	−0·31	0·40
11	3·3883	245·8	0·0435	0·74	(1775)	—	—	0·26
12	3·2883	326·8	0·01844	0·77	1764	0·879	−0·28	0·13
13	3·9651	408·3	0·03894	0·73	(1799)	—	—	0·21
14	3·9651	408·3	0·03914	0·73	1808	0·889	−0·31	0·21
15	5·1006	543·3	0·0956	0·71	(1764)	—	—	0·35
16	4·5154	473·9	0·0632	0·72	(1803)	—	—	0·27
17	4·5154	559·0	0·03898	0·73	(1778)	—	—	0·18
18	4·5154	728·7	0·01680	0·78	(1775)	—	—	0·10
19	4·5154	834·7	0·01001	0·81	1744	—	—	0·07
20	4·5154	944·5	0·00607	0·86	1803	0·897	−0·32	0·05

TABLE 1. Experimental conditions and derived parameters for the samples used in this work

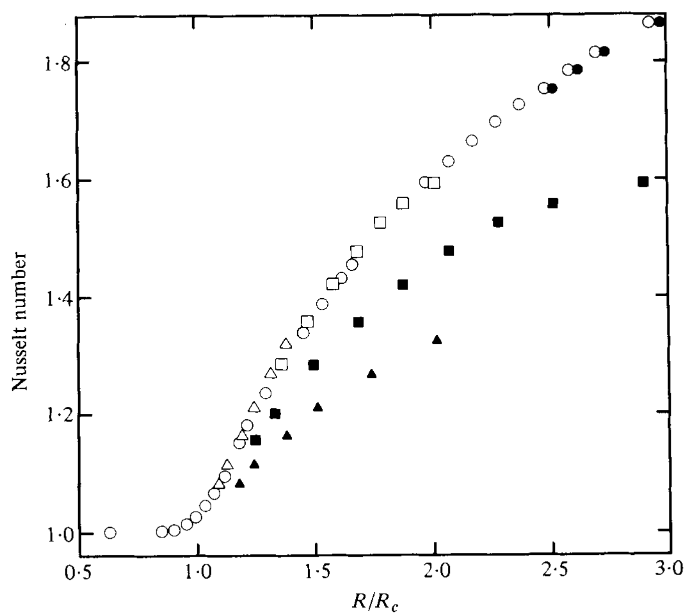

FIGURE 1. Nusselt numbers as a function of the reduced Rayleigh numbers R/R_c. ○, ●, $Q_c = 0·05$; □, ■, $Q_c = 1·05$; △, ▲, $Q_c = 1·93$. (The parameter Q_c is a measure of the extent of departures from the Oberbeck–Boussinesq approximation.) For the open symbols, R/R_c was evaluated at the static temperatures at the midplane of the cell, R_2, R_{c2}. For the solid symbols, R/R_c was evaluated at the cold (top) end temperature of the cell, R_0/R_{c0}.

R_0/R_{c0}	N
0·6283	1·0012
0·8547	0·9989
0·9018	1·0027
0·9470	1·0127
0·9912	1·0253
1·0325	1·0443
1·0718	1·0674
1·1091	1·0942
1·1444	1·1245
1·1816	1·1519
1·2189	1·1798
1·2561	1·2075
1·2933	1·2358
1·3305	1·2642
1·3696	1·2898
1·4087	1·3156
1·4497	1·3389
1·4907	1·3624
1·5317	1·3863
1·5746	1·4079
1·6155	1·4322
1·6584	1·4543
1·7012	1·4765
1·7907	1·5169
1·8820	1·5558
1·9751	1·5937
2·0701	1·6306
2·1688	1·6640
2·2692	1·6965
2·3735	1·7262
2·4814	1·7533
2·5853	1·7853
2·6948	1·8127
2·9228	1·8624
3·2188	1·9203

TABLE 2. Measured Nusselt numbers N and reduced Rayleigh numbers R_0/R_{c0} for sample 20 ($Q_c = 0{\cdot}05$). R_0/R_{c0} was evaluated at T_{s0}, and R_{c0} was taken to be 1803

5. Results

The temperature T_2 at the top of the cell and the ^{4}He gas pressure P are given in the first and second columns of table 1 for each of the investigated samples. Nusselt numbers were calculated from the applied heat current and the measured $T_2 - T_1$ as described in § 2. The Rayleigh numbers R_0 at the midplane of the cell were calculated using the fluid properties given in § 3 and equation (4.7) for T_{s0}. For sample 20, which comes closest to satisfying the OB approximation, the results are given in table 2 and some of them are plotted as open circles in figure 1.

It is evident from figure 1 that $N(R_0)$ shows some rounding in the vicinity of R_{c0}. This has been discussed in detail elsewhere (Ahlers 1975), and is attributable to slight departures from parallelism of the top and bottom plates of the convection cell.

N_{max}	n	R_{c0}	N_{10}	N_{20}	N_{30}	N_{40}
1·21	2	1803	0·911	−0·402	—	—
1·34	2	1802	0·892	−0·301	—	—
1·46	2	1803	0·897	−0·319	—	—
	3	1803	0·928	−0·409	0·078	—
1·63	3	1810	0·937	−0·443	0·112	—
	4	1807	0·923	−0·396	0·051	0·026

TABLE 3. Least-squares fit parameters of equation (5.1) for sample 20. Only data with $N > 1·09$ were used

Recently, measurements have been made by Behringer & Ahlers (1977) on cells with more uniform heights, and $N(R_0)$ has been found to be sharper by an order of magnitude. The rounding near R_{c0} of the data under discussion here causes some difficulty for the determination of R_{c0}. We obtained R_{c0} by fitting data outside the rounded region to the equation

$$N-1 = \sum_{i=1}^{n} N_{i0}\,\epsilon^i, \tag{5.1a}$$

where

$$\epsilon \equiv R_0/R_{c0}-1. \tag{5.1b}$$

In order to test the reliability of this procedure, the data for sample 20 were fitted over various ranges with $N_{min} \leqslant N \leqslant N_{max}$. To exclude the rounded region, we always used $N_{min} = 1·09$ which is sufficiently large. Results for several n and N_{max} are given in table 3. For $n = 2$, the results are largely independent of N_{max}, and for N_{max} sufficiently large to warrant a fit with $n = 3$ or $n = 4$ the results for R_{c0}, N_{10}, and N_{20} are not changed much by changing n. For a systematic analysis of the data for all samples, we used $n = 2$ and $N_{max} = 1·46$. The results for R_{c0}, N_{10}, and N_{20} are given in table 1. For some of the samples, there were insufficient data for $N > N_{min}$ and in those cases R_{c0} was adjusted until agreement with $N(R_0/R_{c0})$ for sample 20 was obtained near $N = 1·1$. These latter results are given in parentheses in table 1.

We believe that the results for R_{c0}, N_{10}, and N_{20} in table 1 are not influenced measurably by the rounding of $N(R)$ near R_c because they are consistent with measurements made in cells of more uniform height with $\Gamma = 4·72$ and $\Gamma = 2·08$ (Behringer & Ahlers 1977), using liquid helium as the fluid. The results for the more uniform geometries are restricted, however, to small Q, and non-OB samples have not been studied in them.

Table 1 also gives values of $T_1 - T_2$ when $R_0 = R_{c0}$, of the Prandtl number σ, and of Q_c (i.e. the value of Q when $R_0 = R_{c0}$). In figure 2, the results for R_{c0} are plotted as a function of Q_c as open circles. It is evident that R_{c0} is independent of Q_c for the range $Q_c \leqslant 2·7$ of the experiments. This result agrees with the prediction by Busse (1967) that R_{c0} should be independent of Q to first order in the coefficients γ_i (see § 4). In order to show that this experimental result is non-trivial, we have evaluated R_2 (R at $z = \frac{1}{2}$) for all the data, fitted N to equation (5.1 a) with

$$\tilde{\epsilon} = R_2/R_{20}-1 \tag{5.1c}$$

replacing ϵ, and plotted the results for R_{c2} in figure 2 as solid circles. The figure clearly

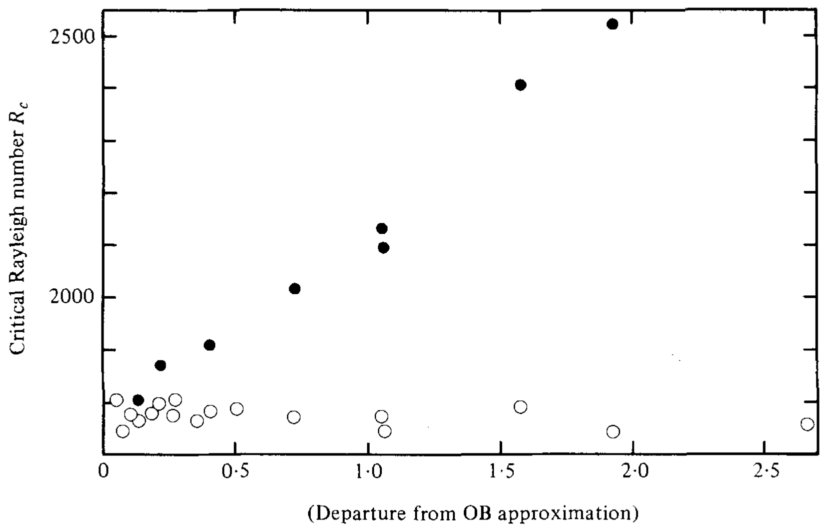

FIGURE 2. Critical Rayleigh number R_c as a function of Q_c. (The value of Q_c is a measure of the extent of departures from the Oberbeck–Boussinesq approximation.) ○, R_c evaluated at the static temperature at the midplane of the cell (for T_{s0}); ●, R_c evaluated at the cold (top) end of the cell (for T_2).

illustrates that the values obtained for R_c are quite sensitive to the value of z used in the data processing, and for the larger Q's only values of z rather close to zero result in the OB values of R_c.

The mean value of R_{c0} is equal to 1775. The major systematic error is due to the uncertainty in h, and is as large as ± 160. The theoretical prediction of R_c for the cylindrical OB system with an aspect ratio near 5·4 is 1730 (Charlson & Sani 1970), in good agreement with the measurements.

For the non-OB system, it is predicted that the transition at R_{c0} should be an inverted bifurcation and that flow in the form of hexagonal cells should be stable for R_0 near R_{c0} (Busse 1967). For the parameters of sample 2 ($\sigma = 0{\cdot}70$, $Q_c = 1{\cdot}93$) we obtain, from (4.8) to (4.10), $-5 \times 10^{-4} \leqslant \epsilon \leqslant 0{\cdot}050$ for the range of stability of hexagons and $\epsilon > 0{\cdot}013$ for the stability of the rolls which are characteristic of the OB system. The range of stability of hexagons is entirely within the rounded region of the data, and therefore the data are not suitable for detecting the predicted inverted bifurcation. We expect the analysis of $N(R_0)$ for $N > 1{\cdot}09$ to pertain to the rolls which are predicted to be stable for $\epsilon > 0{\cdot}013$.

In addition to the data for the OB case (sample 20, $Q_c = 0{\cdot}05$), we have plotted in figure 1 also $N(R_0/R_{c0})$ for sample 7 ($Q_c = 1{\cdot}05$) and for sample 2 ($Q_c = 1{\cdot}93$) as open squares and triangles respectively. These data are seen to agree well with each other and are within our resolution independent of Q. In order to show that a Nusselt number independent of Q is obtained only if R is evaluated at the static temperature near $z = 0$, we also show in figure 1 $N(R_2/R_{c2})$ (i.e. corresponding to $z = \frac{1}{2}$). These results are shown as solid symbols. They show a strong Q dependence.

In order to represent the contents of figure 1 in a more quantitative manner, we have plotted in figure 3 the values of N_{10}, N_{12}, N_{20}, and N_{22} obtained from least-squares

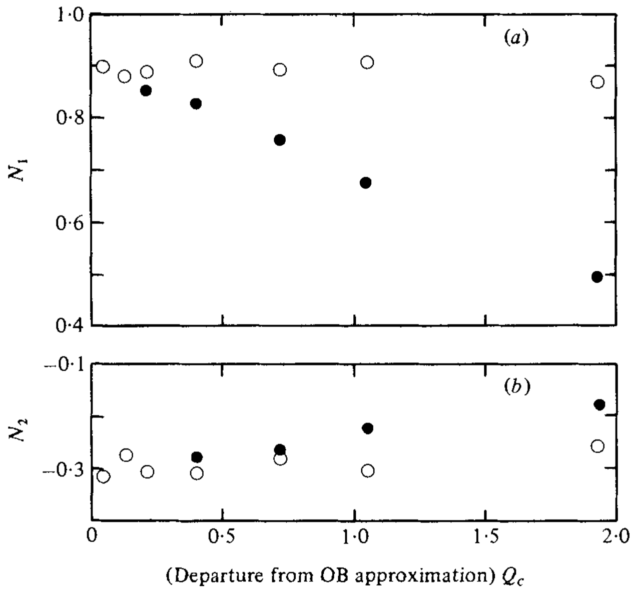

FIGURE 3. The parameters N_1 and N_2, obtained by fitting Nusselt numbers and Rayleigh numbers to equation (5.1), as a function of Q_c. (The value of Q_c is a measure of the extent of departures from the Oberbeck–Boussinesq approximation.) Open symbols were obtained by fitting with R and R_c evaluated at the static temperature at the midplane of the cell (for T_{s0}); solid symbols were obtained by fitting with R and R_c evaluated at the cold (top) end of the cell (for T_2).

fits to (5.1) with $n = 2$ and $N_{\max} = 1{\cdot}45$. The open symbols are N_{10} and N_{20} and were obtained by fitting to (5.1*a*) with ϵ given by (5.1*b*). The solid symbols are N_{12} and N_{22}, and were obtained by fitting to (5.1*a*) with ϵ replaced by $\tilde{\epsilon}$ as given by (5.1*c*). Again it is clear that N_{10} is within experimental scatter independent of Q, whereas N_{12} is strongly Q dependent. For N_2 the experimental information is not quite as definitive, but again N_{20} is more nearly constant than N_{22}.

The best values of N_1 and N_2 in the OB limit are obtained from the analysis of sample 20. They are $N_1 = 0{\cdot}90 \pm 0{\cdot}02$ and $N_2 = -0{\cdot}32 \pm 0{\cdot}02$. Since these results were obtained by fitting to (5.1) which is a truncated expansion for $N-1$, the data were also fitted to the function

$$(N-1)\,R/R_c = \tilde{N}_1\,\epsilon + \tilde{N}_2\,\epsilon^2.$$

If the truncation has a negligible effect, we expect $\tilde{N}_1 = N_1$ and $\tilde{N}_2 = N_1 + N_2$. The result was $\tilde{N}_1 = 1{\cdot}02 \pm 0{\cdot}02$ and $\tilde{N}_2 = 0{\cdot}22 \pm 0{\cdot}02$. It is apparent that the data do not yield very quantitative information for the coefficient of the ϵ^2 term. Our best estimate for the initial slope would be somewhere between N_1 and $\tilde{N}_1$, and about equal to $0{\cdot}96 \pm 0{\cdot}06$. For the laterally infinite system, this slope has been calculated by Schlüter *et al.* (1965), and for $\sigma = 0{\cdot}86$ is equal to $1{\cdot}428$. Measurements at large Prandtl numbers and for an aspect ratio much larger than ours by Koschmieder & Pallas (1974) and by Rossby (1969) agree rather well with the prediction. The small value of the initial slope obtained in this work is attributable to the small aspect ratio of the experimental cell. This has been discussed in more detail elsewhere (Behringer & Ahlers 1977).

6. Summary

In this paper experimental data were presented for convective heat transport in horizontal layers of ^{4}He gas which were heated from below. The convection cell had cylindrical symmetry, and the aspect ratio $\Gamma \equiv D/2h$ (D = diameter, h = height) was equal to 5·4. By choosing different temperatures and pressures, the extent Q of departures of the system from the approximation of Oberbeck (1879) and of Boussinesq (1903) was varied. The results were analysed in terms of the theoretical predictions by Busse (1967). None of the measurements revealed the existence of the predicted inverted bifurcation at R_c which is expected to be associated with the flow of hexagonal symmetry near R_c. Instead, the Nusselt number was rounded over a narrow range of R. We attribute this to imperfections in the geometry of the cell. For the maximum value of Q achieved during the experiment, the predicted range of stability of hexagonal flow fell within the rounded region, and therefore the data do not give any information about the existence of the inverted bifurcation.

Outside the rounded region, the results for $N(R)$ were fitted to a polynomial in $\epsilon \equiv R/R_c - 1$. This fit yielded estimates of R_c and of the initial slope N_1 of N *vs.* R. It was found that both N_1 and R_c were independent of Q if R was evaluated at the static temperature T_{s0} at the midplane of the cell. This result agrees with the prediction by Busse (1967). In order to show that only a fit using $R(T_{s0})$ gives Q-independent values of R_c and N_1, the analysis was carried out also using $R(T_2)$, where T_2 is the temperature at the cold end of the cell. In that case, both R_c and N_1 were found to be strongly Q-dependent.

The values found for R_c in the limit $Q = 0$ agreed within experimental uncertainties with the theoretical result for a laterally finite system with $\Gamma = 5{\cdot}4$ (Charlson & Sani 1970), but had insufficient accuracy to distinguish between the finite Γ value of R_c and the one appropriate for $\Gamma = \infty$. The initial slope N_1 was less than the theoretical value for $\Gamma = \infty$ (Schlüter *et al.* 1965), but consistent with measurements for other finite aspect ratios (Behringer & Ahlers 1977).

REFERENCES

Ahlers, G. 1971 Heat capacity near the superfluid transition in ^{4}He at saturated vapor pressure. *Phys. Rev.* A **3**, 696–716.

Ahlers, G. 1974 Low temperature studies of the Rayleigh–Bénard instability. *Phys. Rev. Lett.* **33**, 1185–1188.

Ahlers, G. 1975 The Rayleigh–Bénard instability at helium temperatures. In *Fluctuations. Instabilities, and Phase Transitions* (ed. T. Riste), pp. 171–193. Plenum.

Ahlers, G. 1978 Thermal conductivity of ^{4}He vapor as a function of density. *J. Low Temp. Phys.* **31**, 429–439.

Becker, E. W., Misenta, R. & Schmeissner, F. 1954*a* Viscosity of gaseous He^3 and He^4 between 1·3 °K and 4·2 °K. *Phys. Rev.* **93**, 244.

Becker, E. W., Misenta, R. & Schmeissner, F. 1954*b* Die Zähigkeit von gasförmigem He^3 und He^4 zwischen 1·3 °K und 4·2 °K. *Z. Phys.* **137**, 126–136.

Behringer, R. P. & Ahlers, G. 1977 Heat transport and critical slowing down near the Rayleigh–Bénard instability in cylindrical containers. *Phys. Lett.* A **62**, 329–331.

Boussinesq, J. 1903 *Théorie Analytique de la Chaleur*, vol. 2. Paris: Gauthier–Villars.

Busse, F. H. 1962 Dissertation, University of Munich. [English translation by S. H. Davis, *Rand Rep. LT*-66-19, Rand Corp., Santa Monica, California.

BUSSE, F. H. 1967 The stability of finite amplitude cellular convection and its relation to an extremum principle. *J. Fluid Mech.* **30**, 625–649.

CHARLSON, G. S. & SANI, R. L. 1970 Thermoconvective instability in a bounded cylindrical fluid layer. *Int. J. Heat Mass Transfer* **13**, 1479–1496.

DAVIS, S. H. & SEGEL, L. A. 1968 Effects of surface curvature and property variation on cellular convection. *Phys. Fluids* **11**, 470–476.

DUBOIS, M., BERGE, P. & WESFRIED, J. 1978 Non-Boussinesq convective structures in water near 4 °C. *J. Phys.* **39**, 1253–1257.

HIRSCHFELDER, J. O., CURTISS, C. F. & BIRD, R. B. 1954 *Molecular Theory of Gases and Liquids.* Wiley.

HOARD, C. Q., ROBERTSON, C. R. & ACRIVOS, A. 1970 Experiments on cellular structure in Bénard convection. *Int. J. Heat Mass Transfer* **13**, 849–855.

JOSEPH, D. D. 1971 Stability of convection in containers of arbitrary shape. *J. Fluid Mech.* **47**, 257–282.

KELLER, W. E. 1969 *Helium*-3 *and Helium*-4. Plenum.

KERRISK, J. F. & KELLER, W. E. 1969 Thermal conductivity of fluid He^3 and He^4 at temperatures between 1·5 and 4·0 K and for pressures up to 34 atm. *Phys. Rev.* **177**, 341–351.

KOSCHMIEDER, E. L. & PALLAS, S. G. 1974 Heat transfer through a shallow, horizontal convecting fluid layer. *Int. J. Heat Mass Transfer* **17**, 991–1002.

OBERBECK, A. 1879 Über die Wärmeleitung der Flüssigkeiten bei der Berücksichtigung der Strömungen infolge von Temperaturdifferenzen. *Ann. Phys. Chem.* **7**, 271–292.

PALM, E., ELLINGSEN, T. & GJEVIK, B. 1967 On the occurrence of cellular motion in Bénard convection. *J. Fluid Mech.* **30**, 651–661.

ROSSBY, H. T. 1969 A study of Bénard convection with and without rotation. *J. Fluid Mech.* **36**, 309–335.

SCHLÜTER, A., LORTZ, D. & BUSSE, F. 1965 On the stability of steady finite amplitude convection. *J. Fluid Mech.* **23**, 129–144.

SOMERSCALES, E. F. C. & DOUGHERTY, T. S. 1970 Observed flow patterns at the initiation of convection in a horizontal liquid layer heated from below. *J. Fluid Mech.* **42**, 755–768.